JOURNAL OF SOLID STATE CHEMISTRY 62, 26–34 (1986)

Structural Characterization and Ionic Conductivity of Co^{2+}-Stabilized β''-Alumina

S. CHEN,*,[1] D. R. WHITE,*,[2] H. SATO,* J. B. LEWIS,†
AND WILLIAM R. ROBINSON†

**School of Materials Engineering and †Department of Chemistry, Purdue University, West Lafayette, Indiana 47907*

Received April 8, 1985; in revised form July 26, 1985

Single crystals of Co^{2+}-stabilized β''-alumina were synthesized by a flux growth technique using Bi_2O_3 as the flux and subsequent X-ray crystallographic studies showed that the Co^{2+} ions substitute only at the Al(2) sites. Optical absorption spectroscopic measurement also supports the concept that the dopant ions are in distorted tetrahedral environment. Co^{2+}-doped β-alumina crystals were made by a skull melting technique. Chemical analysis of these two materials indicated that the Co^{2+} ion concentration may be important in the formation of one phase over the other. The temperature-dependent ionic conductivity of Co^{2+}-stabilized β''-alumina, Co^{2+}-doped β-alumina, and undoped β-alumina has been measured and compared between 25 and 450°C. The detailed conductivity analysis was made by a phase-synchronous detection system in the frequency range 100 Hz–10 MHz. The conductivity is highest in the stabilized β''-alumina and lowest in the undoped β-alumina. For Co^{2+}-doped β-alumina, a slight bend in the conductivity at around 200°C is noted. The analysis of the conductivity and the effect of the dopant Co^{2+} ions on the resulting conductivity is discussed.

Introduction

In the β-alumina family, both β- and β''-aluminas have been investigated quite extensively. With its higher ionic conductivity, however, β''-alumina has emerged as the more important candidate for a solid electrolyte material. When synthesized with a composition of $Na_2O \cdot 5Al_2O_3$, β''-alumina is known to be metastable with respect to β-alumina (*1, 2*). Nevertheless, it can be stabilized by the addition of divalent and monovalent spinel-forming cations such as Mg^{2+} (*3*), Zn^{2+} (*4*), or Li^{+} (*5*), and the location of such cations and their effects on the ionic conductivity have been topics of interest.

The structure of β-alumina type compounds can be regarded as a stacking of two structural units, D (defect) and S (spinel) blocks, so that the structure of a family of β-alumina compounds can be represented by the stacking formula $D(nS)D^*(nS^*)$ with $n = 0, 1, 2, \ldots$ (*6, 7*). Here, n indicates the number of the S block and hence the period of the compound. The D^* and S^* blocks are the same as D and S, but rotated by 180° with respect to the c axis. The ordinary β-alumina correspond to the structure with $n = 1$. On the other hand, β''-alumina-type compounds can be described as

---

[1] Present address: Research Laboratories, Eastman–Kodak Company, Rochester, N.Y. 14650.

[2] Present address: Lanxide Corporation, Newark, Del. 19711.

0022-4596/86 $3.00

$[D''(nS)]_3$, where D″, with the rhombohedral stacking symmetry, corresponds to D of β-alumina. For normal β''-alumina, the structure is again represented by the $n = 1$ compound. The structures of β- and β''-aluminas differ primarily in the stacking of close packed oxygen layers at both sides of the conduction layers with the S block being common to both materials. The unit S block is equivalent to the unit cell (in the c direction) of spinel. In normal spinels such as $MgAl_2O_4$ or $CoAl_2O_4$, it has been found that the trivalent Al^{3+} ions prefer the octahedral sites, and the divalent ions are found only in the tetrahedral sites. Interestingly, Al^{3+} is found in both the octahedral and tetrahedral sites of the S block in undoped β- and β''-aluminas. However, the aversion of Al^{3+} for the tetrahedral sites is observed experimentally in such materials as Ni^{2+}-doped β-alumina (*8*) and Mg^{2+}-stabilized β''-alumina (*3, 9*) where the divalent cations preferentially substitute for the Al^{3+} only in the tetrahedral Al(2) sites of the S block. In addition, McWhan *et al.* (*10*) have reported the difficult nature of trying to grow pure β-alumina without any divalent metal ion impurity inclusions. This substitution of divalent ions for trivalent ions results in a decrease of the excess positive charge in the S block. Correspondingly, a decrease in the excess negative charge occurs in the D block (*7*). In β-alumina, this fact has been attributed to the removal of extra oxygens in the conduction layer in order to achieve local charge neutrality (*11*). In β''-alumina, however, the charge compensation mechanism has been correlated to the incorporation of excess sodium ions into the conduction plane (*12*). Also, the incorporation of excess sodium ions was found necessary to explain the decomposition characteristic of Fe-stabilized β''-alumina (*13*).

Since both β- and β''-aluminas can accommodate divalent metal ions in the S block and this substitution can in turn affect the chemistry of the D block as well as the conduction plane, we were interested in examining both the structural and electrical changes in these materials as a function of the divalent ions. Although both doped β-alumina and stabilized β''-aluminas are known, detailed structural studies of these materials containing the same divalent metal ions have not been reported. Recently we have succeeded in controlling the amount of divalent metal ions introduced into the S block of these materials so that both divalent metal-doped β-alumina and divalent metal-stabilized β''-alumina uncontaminated with other phases can be synthesized. In this paper we report a systematic analysis of the structural characteristics (*14*) and the ionic conductivity (*15*) for β- and β''-aluminas in which both contain Co^{2+} as the ternary cation.

Experimental

Crystal Growth

Single-phase, single-crystal Co^{2+}-stabilized β''-alumina (hereafter abbreviated as Co-β''), was prepared following the procedure reported by McWhan *et al.* (*10*). A mixture with the molar proportions $1Na_2O : 1.86Al_2O_3 : 0.45CoO$ was placed in a 100-ml Pt crucible with Bi_2O_3 as the flux. This mixture was heated in air to 1300°C and then slowly cooled at 2°/hr to 750°C before the furnace was switched off. The resulting Co-β'' crystals were extracted from the flux in a hot HCl solution. Hexagonal-shaped crystals 10 mm in diameter by

TABLE I

X-RAY FLUORESCENCE QUANTITATIVE ANALYSIS OF M^{2+} β-ALUMINAS

	Weight %		
	$[Na^+]$	$[Al^{3+}]$	$[Co^{2+}]$
Co^{2+}-Doped β-alumina	6.30	46.86	1.68
Co^{2+}-Stabilized β''-alumina	6.78	43.80	5.94

1 mm in thickness have been obtained. Single crystalline Co^{2+}-doped β-alumina was prepared by the skull melting technique as described in previous publications (*8*, *16*). Results of the X-ray fluorescence analysis of these two systems are shown in Table I. Electron diffraction patterns on crushed crystals from either sample revealed the presence of only single phased material. Since Co^{2+}-doping imparts a deep blue color to β-alumina compounds, the room temperature absorption spectra for both Co^{2+}-β''- and Co^{2+}-doped β-alumina (Fig. 1) were recorded from 250 to 700 nm on a Cary 17D spectrophotometer using ground single crystals, suspended in Nujol between two quartz plates. Both compounds exhibited the same absorption spectrum and the triplet centered around 600 nm is attributed to Co^{2+} ions in pseudotetrahedral environments. This *d–d* transition has been assigned by Akridge *et al.* as $^4T_1(^4p) \leftarrow {}^4A_2(^4F)$, first observed in polycrystalline sintered Co^{2+}-doped β-alumina (*17*).

Structure Refinement

For the structural study (*14*), a blue optically clear parallelepiped Co-β'' crystal with the approximate dimensions 0.45 × 0.30 × 0.05 mm was mounted on a glass fiber. Initial Weissenburg photographs of several $00l$ levels showed systematic absences satisfying the relationship $-h + k + l = 3n$, consistent with the space group $R\bar{3}m$ as reported by others (*9*). The Co-β'' crystal was then placed on an Enraf–Nonius CAD-4 X-ray diffractometer and using Ni-filtered Cu$K\alpha$ radiation, the least-squares unit cell dimensions were determined to be a = 5.6153(9) Å and c = 33.712(5) Å, by refinement of the settings of 24 carefully centered reflections. Intensity data from a hemisphere of reciprocal space was collected in the region $6° < 2\theta < 120°$ with Miller indices ranging from $-6 \leq h \leq 6$; $-6 \leq k \leq 6$; $-35 \leq l \leq 0$. This resulted in 914 reflections, which were then corrected for absorption, background and Lorentz-polarization effects. Upon averaging for equivalent reflections and excluding those with $F_o^2 \leq 3\sigma F_o^2$, based on the deviation from average or counting statistics of unique reflections, a total of 201 unique reflections was obtained. Scattering factors for neutral atoms, corrected for real and imaginary anomalous dispersion, were used in the full matrix least-squares structural refinement, in which the factor $\Sigma\omega(|F_o| - |F_c|)^2/\Sigma\omega(|F_o|)^2$ was minimized.

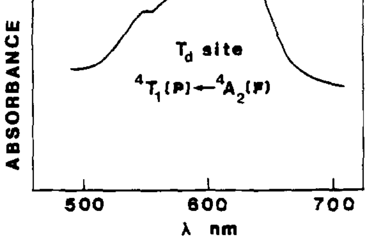

FIG. 1. Visible absorption spectrum of Co^{2+} ions in Co^{2+}-stabilized β''-alumina or Co^{2+} doped β-alumina.

No crystallographic study on the Co^{2+}-doped β-alumina system was carried out as this structure is already known (*18*).

The initial positions for aluminum and oxygen were taken from the report by Bettman *et al.* (*3*). A preliminary refinement using just isotropic temperature factors resulted in a residual $R = 0.464$. The substitution of cobalt as one-third of the content at the Al(2) site (fraction determined by using the ideal formula) resulted in $R = 0.524$. Even though the residual went up slightly when Co was added to this position, the placement of Co in other tetrahedral or octahedral aluminum sites led to nonconvergent results. With the use of anisotropic temperature factors in subsequent refinements, the residual decreased sharply.

The locations of sodium atoms in the conduction plane were refined by several approaches. Sodium was first placed only in the ideal Beevers–Ross position (6*c*), but the resulting difference electron density map indicated that a displacement from this position was reasonable. However, putting sodium only in the displaced positions (18*h*) increased the residual. Ultimately, assigning sodium to both the 6*c* and 18*h* positions and making the sodium positions anisotropic reduced the residual to $R = 0.068$. At this stage the occupancies of the sodium sites were refined, holding all other parameters constant. A difference electron density contour map of the conduction layer revealed the highly anisotropic nature of the sodium atoms, whose triangular, liquidlike disordered feature resembles that reported by Brown *et al.* (*4*).

In the final stages of refinement, the thermal parameters of the cobalt were constrained to follow those of aluminum at the Al(2) site and then their multiplicities at this position were also allowed to vary independently, resulting in a final $R = 0.065$. It is interesting to note that the decrease in multiplicities of both atoms at the Al(2) site implies incomplete occupancy, i.e., aluminum vacancies, at this position in the Co-β'' structure. Based on this structural refinement, the empirical formula is $Na_{1.82}Al_{10.2}Co_{0.701}O_{17}$. However, a recent EXAFS study which examined the local structure around Co^{2+} (*19*), showed that in Co-β'' the average Co–O bond length (1.95 Å) is significantly longer than the averaged *M*(2)–O distance (1.838 Å, Table IV). Such a structural disorder may introduce a degree of uncertainty during the refinement of the occupancy at the Al(2) site.

The occupancy of the O(5) position (bridging oxygen in the conduction plane) was also independently refined. The reasoning behind this was that the oxygens in the conduction layers are not in the close-packed arrangement and are more susceptible to nonstoichiometry, especially with the change in stoichiometry of the S block by the addition of divalent ions. This refinement ($R = 0.064$) suggests an occupancy at O(5) that is less than the full occupancy by five standard deviations [0.078(1) as opposed to the ideal 0.08333, Table II]. However, these two occupancy values are statistically equivalent based on Hamilton's test in which the level of significance $\alpha = 0.005$ (*20*). In other words, neither model is preferrable. Although a decrease in oxygen occupancy at the O(5) site has not been reported in the literature, a lower value suggests that less negative charge is present in the conduction layer, possibly to compensate for the decreased positive charge in the spinel block. If this site is not fully occu-

TABLE II

STRUCTURAL PARAMETERS FOR Co^{2+} STABILIZED β''-ALUMINA

Atom	Al(1)	Al(2)	Co	Al(3)	Al(4)	O(1)	O(2)	O(3)	O(4)	O(5)	Na(1)	Na(2)
Wyckoff position	18*h*	6*c*		6*c*	3*a*	18*h*	18*h*	6*c*	6*c*	3*b*	6*c*	18*h*
Theor. occup.	0.5	0.16667	—	0.16667	0.08333	0.5	0.5	0.16667	0.16667	0.08333	0.16667	0.5
Refined occup.	—	0.093(1)	0.0584(6)	—	—	—	—	—	—	0.078(1)	0.051(2)	0.100(2)
x	0.3347(3)	0		0	0	0.1535(4)	0.1631(3)	0	0	0	0	−0.063(2)
z	0.0711(1)	0.3500(1)		0.4502(1)	0	0.0343(1)	0.2353(1)	0.2958(2)	0.966(2)	0.5	0.176(1)	0.1713(3)
U_{11}	0.0234(9)	0.0219(8)		0.0249(9)	0.021(1)	0.029(1)	0.028(2)	0.022(2)	0.024(2)	0.006(1)	0.130(1)	0.076(6)
U_{22}	0.0242(6)	U_{11}		U_{11}	U_{11}	0.032(2)	0.023(2)	U_{11}	U_{11}	U_{11}	U_{11}	0.150(2)
U_{33}	0.0146(7)	0.011(1)		0.015(1)	0.014(2)	0.017(2)	0.015(2)	0.027(3)	0.016(3)	0.024(5)	0.160(3)	0.021(5)
U_{12}	U_{11}	U_{11}		U_{11}	U_{11}	U_{22}	U_{22}	U_{11}	U_{11}	U_{11}	U_{11}	U_{22}
U_{13}	$2U_{23}$	0		0	0	$\frac{1}{2}U_{23}$	$\frac{1}{2}U_{22}$	0	0	0	0	$\frac{1}{2}U_{23}$
U_{23}	0.000(3)	0		0	0	−0.002(2)	−0.001(2)	0	0	0	0	0.37(6)

The form of the anisotropic thermal parameter is $\exp[-2\pi^2(h^2a^{*2}U_{11} + k^2b^{*2}U_{22} + l^2c^{*2}U_{33} + 2hka^*b^*U_{12} + 2hla^*c^*U_{13} + 2klb^*c^*U_{23})]$.

TABLE III

INTERATOMIC DISTANCES FOR Co^{2+}-STABILIZED β''-ALUMINA (IN Å)

Al(1) octahedron	
-O(1)	1.997(1) × 2
-O(2)	1.840(1) × 2
-O(3)	1.972(2) × 1
-O(4)	1.840(1) × 1
Al(2) tetrahedron–spinel block	
-O(2)	1.846(1) × 3
-O(3)	1.829(3) × 1
Al(3) tetrahedron–bridging	
-O(2)	1.773(1) × 3
-O(5)	1.681(1) × 1
Al(4) octahedron	
-O(1)	1.888(1) × 6
Na(1)	
-O(2)	2.56(2) × 3
-O(4)	2.66(2) × 1
-O(5)	3.256(2)
-Na(2)	0.597(2)
Na(2)	
-O(2)	2.564(7)
-O(4)	2.594(7)

pied, the empirical formula would become $Na_{1.82}Al_{10.2}Co_{0.701}O_{16.9}$.

The final atomic position and thermal parameters are listed in Table II and the interatomic distances are presented in Table III. A table of observed and calculated structure factors is available in Ref. (*14*) or on request from W.R.R., one of the authors.

Conductivity Measurements

Conductivity measurements were taken via a phase-synchronous detection technique (*15, 21, 22*) employing a Hewlett–Packard 3040A network analyzer. The system is fully automated under the control of a Hewlett–Packard 9836 minicomputer which also provides data acquisition analysis. This setup is capable of providing impedance measurement from 100 Hz to 10 MHz over the temperature range 25–600°C. Samples were cut from single crystals into parallelopipeds with platinum contacts sputtered onto two opposite sides parallel to the *c* axis, i.e., perpendicular to the conduction plane. All samples were allowed to bakeout in the test cell at 600°C for 3 h in vacuum (~10 mTorr) prior to measurement.

Data analysis was carried out using a least-squares fitting routine (*21*) in which the d.c. resistance of the crystal is one of the fitting parameters. The fitting function is based in part on an equivalent circuit model representing the electrical response of the sample. The model giving the best fits (Fig. 2) consists of a resistor *R* and a non-Debye capacitor *C′* (*22*), in parallel with a Debye capacitor *C*. In this model the resistor represents the d.c. resistance of the material, while the non-Debye capacitor represents the combined dielectric response of the conduction plane and interfacial capacitance of the electrode/electrolyte interface. In other words, this branch represents the dielectric response of the D block. The parallel capacitor is thought to represent the dielectric response of the S block. Since spinel compounds are in general good insulators, i.e., low loss dielectrics, the assumption that this portion of the material has a Debye-like response appears reasonable.

Discussion

The location of the divalent metal ion in Co^{2+}-β'' has been established by least-squares structural refinement and absorption spectroscopy to be the (distorted) tetrahedral Al(2) site in the S block of the β''-alumina structure. This is the original tetrahedral site found in normal spinel.

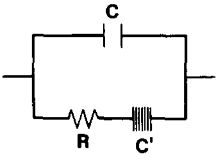

FIG. 2. Equivalent circuit for single crystalline β-aluminas, consisting of a capacitor *C*, in parallel with a resistor *R*, and a non-Debye capacitor *C′*.

TABLE IV

COMPARISON OF TETRAHEDRAL ALUMINUM–OXYGEN DISTANCES (Å) IN β-ALUMINA COMPOUNDS

	Sum of atomic radii (*25*)	β-alumina (*26*)	Co^{2+}-doped β-alumina (*18*)	Co^{2+}-stabilized β″-alumina (this work)
Al(3)–O(2) × 3		1.768	1.772	1.773
Al(3)–O(5) × 1		1.677	1.723	1.681
Average	1.74	1.723	1.759	1.727
Al(2)–O(1) × 3		1.801	1.811	1.846
Al(2)–O(3) × 1		1.809	1.814	1.829
Average	1.74	1.803	1.812	1.838

Such a finding matches those of other M^{2+}-stabilized β″-aluminas, where $M^{2+} = Mg^{2+}$ (*23*), Zn^{2+} (*4*), and Ni^{2+} (*8*). Similarly, in the case of Co^{2+}-doped β-alumina, Dernier and Remeika (*18*) have also determined that the divalent metal ion is situated in the equivalent Al(2) position in the S block of the β-alumina structure. The identical absorption spectra of these two forms of β-aluminas provide the added support that the Co^{2+} ion is indeed in that tetrahedral site. As pointed out earlier, the observation that Co^{2+} goes only into this tetrahedral site is not surprising in view of the fact that the S block corresponds to the unit cell of (normal) spinel such as $CoAl_2O_4$, where the Co^{2+} is also found only in tetrahedral cavities (*24*).

Several tetrahedrally coordinated aluminum–oxygen distances are shown in Table IV. There are two types of tetrahedrally coordinated Al sites in β-alumina compounds, namely Al(2) in the S block, and Al(3) in the D block. Because of the inequivalent oxygen positions around each aluminum site, and especially in the D block, both the individual Al–O and their averaged distances are shown. A reference Al–O distance, based on the Al and O atomic radii taken from Shannon and Prewitt (*25*) is also included. For the Al(3)–O distances in the various β-alumina compounds, the averaged value shows only minor variations from the reference Al–O distance. This is not unexpected since the Co does not substitute at the Al(3) site and any structural changes would only be indirect. On the other hand, the average Al(2)–O distance in these compounds show major variations. Even in pure β-alumina (*26*), the value of 1.809 Å is significantly larger than the reference distance of 1.74 Å, suggesting that this tetrahedral cavity is too large for the trivalent Al^{+3} ion (radius = 0.39 Å). Doping with a small amount of the larger divalent Co^{2+} cation (radius = 0.58 Å) results in an expected increase to 1.812 Å (Co^{2+}-doped β-alumina). With an even larger amount of substitution, this distance in Co-β″ increases to 1.838 Å. While it is possible that divalent ion doping at the Al(2) site may relieve local lattice strain in the S block (*12*), it is as yet not clear why it is the β″-alumina structure that can accommodate the larger concentration of the dopant ion. Interestingly, a plot of the Al(2)–O distance vs the ratio of the occupancy of Co to Al at the Al(2) site, for pure β-alumina, Co^{2+}-doped β-alumina (*18*) and Co-β″, shows a surprisingly linear relationship reflecting the similarity of the S block in both the β- and β″-alumina lattice. Hence, this proportionality relationship may be of use towards such studies as the synthesis of other cation

TABLE V

COMPARISON OF THE DIVALENT METAL ION CONTENT IN β- AND β″-ALUMINA COMPOUNDS

Compound	M^{2+}	($[M^{2+}/[\mathrm{Al}]$)	Method of analysis	Ref.
β″-Alumina				
$Na_{4.7}Al_{30.4}Mg_{2.6}O_{51}$	Mg	0.085	Neutron diffraction	(*9*)
$Na_{1.67}Al_{10.33}Mg_{0.67}O_{17}$	Mg	0.065	Chemical analysis	(*4*)
$Na_{1.71}Al_{10.29}Mg_{0.71}O_{17}$	Mg	0.069	(Neutron activation), X-ray structural determination	(*23*)
$Na_{1,57}Al_{10.43}Zn_{0.57}O_{17}$	Zn	0.055	Chemical analysis	(*4*)
$Na_{1.82}Al_{10.1}Co_{0.70}O_{17}$	Co	0.069	X-Ray structural determination	This work
Co^{2+}-stabilized β″-alumina	Co	0.06	Chemical analysis	(*10*)
Ni^{2+}-stabilized β″-alumina	Ni	0.084	X-Ray fluorescence	*8*
β-Alumina				
$K_{2.68}Al_{21.4}Co_{0.6}O_{34+x}$	Co	0.028	X-ray structural refinement	*18*
Co^{2+}-doped β-alumina	Co	0.016	X-Ray fluorescence	This work
Ni^{2+}-doped β-alumina	Ni	0.036	X-Ray fluorescence	*8*

doped β-aluminas once the composition of the analogous cation stabilized β″-alumina material is known.

The compositional analysis of the two forms of β-aluminas doped with Co^{2+} shows that the concentration of the substituted divalent metal ion is significantly higher in the β″ form. Since these two phases can be selectively synthesized, the Co^{2+}-concentration in the S block may be a factor that controls the stability of one form over the other. Indeed, it has been reported that Co^{2+}-doped β-alumina can be grown by a flux growth technique at 1300°C, without any inclusions of Co^{2+} stabilized β″-alumina, if the nominal Co/Al molar ratio is kept below 0.009 (*18*). The significance of this ratio has been explored and Table V lists the $[M^{2+}]/[\mathrm{Al}]$ molar ratio for the various divalent metal-doped and divalent metal-stabilized β-alumina compounds. Even allowing room for the differing amount of errors in accuracy associated with the various analytical techniques used to characterize these materials, it would appear that the amount of substituted divalent metal ions is lower in the doped β-alumina structure.

The concentration of Co^{2+}, however, may not be the only phase-controlling factor. As early as 1962, Thery and Briançon (*27*) pointed out the irreversible transformation of β″-alumina to β-alumina when

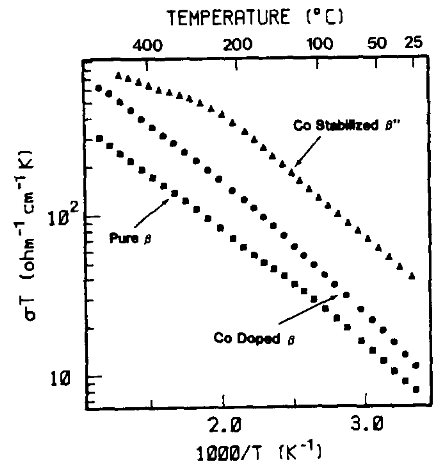

FIG. 3. Conductivity plot comparing Co^{2+}-stabilized β″-alumina, Co^{2+}-doped β-alumina, and pure β-alumina.

TABLE VI

CONDUCTIVITY DATA OF β-ALUMINA COMPOUNDS

Compound	E_a (eV)	σ_0 (Ω^{-1} cm^{-1} K)	$\sigma_{25°C}$ (Ω^{-1} cm^{-1})
Pure β-alumina	0.142 ± 0.002	2100 ± 13	0.028
Co^{2+}-Doped β-alumina	0.139 ± 0.001^a	4023 ± 106^a	0.039
	0.172 ± 0.002^b	9379 ± 626^b	
Co^{2+}-Stabilized β''-alumina	0.060 ± 0.003^a	1816 ± 90^a	0.131
	0.154 ± 0.001^b	15520 ± 581^b	

[a] From high temperature data ($\sim T > 200°C$).

[b] From low temperature data ($\sim T < 200°C$).

Note. The data are broken into two parts due to the bending in the conductivity curve of both the Co^{2+}-doped β-alumina and Co^{2+}-stabilized β''-alumina.

heated to 1500°C. We have followed the structural changes that can take place, at $\frac{1}{2}$-hr intervals, via X-ray powder diffraction, on crushed single crystalline Co-β'' (grown by cooling from 1300°C) that was heated in sealed Pt foil at 1600°C. A slow transformation from β''- to β- to α-alumina was observed in the diffraction peaks. Since the final product was colorless corundum, this overall transformation reaction presumably involves the loss of CoO and Na_2O (*27, 28*). Nevertheless, the possibility that even stabilized β''-alumina is yet a metastable, low temperature form of β-alumina cannot be denied. Our experience with the skull melting crystal growth of β-alumina containing Co (*16*) showed that upon slow cooling from its melting point of approximately 1950°C, the portion that crystallizes first consist primarily of the doped β-alumina phase, while the volume that freezes last (i.e., lower melting point) contains predominantly the stabilized β''-alumina phase. Thus the temperature used in crystal growth may also play a critical role in controlling the formation of the β- or β''-alumina phase.

The result of the conductivity measurements of Co-β'' is shown in Fig. 3 and in Table VI. For comparison, data for Co^{2+}-doped β-alumina and pure β-alumina are also given. As can be seen, the Co-β'' has the highest conductivity of the materials tested over the entire temperature range, with a value of 0.131 Ω^{-1} cm^{-1} at 25°C. In fact, this value is one of the highest reported for all β''-alumina compounds. The non-Arrhenius behavior of this compound is similar to that observed for Mg^{2+}-stabilized β''-alumina (*22*) and has been attributed to the development of ordering between the ions and vacancies in the conduction plane (*23, 29, 30, 31*). However, this behavior is still not well understood.

The differences in conductivity of these compounds (doped, undoped) may be correlated in part with the variation in the amounts of the dopant ions, ranging from 0% in the undoped β-alumina to 5.94% in Co^{2+} stabilized β''-alumina. The effect of this doping is thought to result in the removal of excess bridging oxygen ions in the conduction plane (*32*), thus providing a lower resistance path for ionic diffusion. Even though the present structural analysis of the occupancy at the O(5) site is not conclusive, the higher conductivity of the stabilized β''-alumina may in part be due to a further removal of the bridging oxygen ions in the conduction plane. Such an effect may, however, be minor when compared to the overall difference in geometry and contour of the conduction pathway between the β- and β''-alumina structure. Along with the increased mobility of conduction ions, the removal of bridging ions can contribute to the formation of short-range order among the conduction ions. It should also be pointed out that the conductivity response of doped β-alumina compounds exhibited a gradual bending in the temperature range 200–300°C. This behavior is currently being studied and will be discussed in more detail in a future publication (*33*).

Acknowledgments

We thank the Monsanto Fund and the NSF-MRL program at Purdue University (DMR 80-20249) for the support of this work, as well as the NSF (Grant CAG-8204994) for providing the X-ray equipment. We also thank Dr. J. B. Bates of Oak Ridge National Laboratories and Dr. Herbert Engstrom of Magnetic Peripherils, Inc. for their help in the development of the phase synchronous detection system.

References

1. N. WEBER AND A. F. VENERO, Ford Motor Company Scientific Research, Technical Report No. SR69-86 (1969).
2. J. D. HODGE, *J. Amer. Ceram. Soc.* **66,** 166 (1983).
3. M. BETTMAN AND C. R. PETERS, *J. Phys. Chem.* **73,** 1774 (1969).
4. G. M. BROWN, D. A. SCHWINN, J. B. BATES, AND W. E. BRUNDAGE, *Solid State Ionics* **5,** 147 (1981).
5. J. D. JORGENSEN, F. J. ROTELLA, AND W. L. ROTH, *Solid State Ionics* **5,** 143 (1981).
6. H. SATO AND Y. HIROTSU, *Mater. Res. Bull.* **11,** 1307 (1976).
7. H. SATO, H. KUWAMOTO, Y. HIROTSU, N. OTSUKA, AND G. L. LIEDL, *Rev. Chim. Miner.* **71**(7), 404 (1980).
8. D. R. WHITE, S. CHEN, H. R. HARRISON, AND H. SATO, *Solid State Ionics* **9&10,** 255 (1983).
9. W. L. ROTH, W. C. HAMILTON, AND S. J. LAPLACA, *Amer. Crystallogr. Assoc. Abstr. Ser. 2* **1,** 169 (1973).
10. D. B. MCWHAN, P. D. DERNIER, C. VETTIER, A. S. COOPER, AND J. P. REMEIKA, *Phys. Rev. B* **17,** 4043 (1978).
11. W. L. ROTH, *J. Solid State Chem.* **4,** 60 (1972).
12. W. L. ROTH, F. REIDINGER, AND S. J. LAPLACA, "Superionic Conductor" (G. H. Mahan and W. L. Roth, Eds.), p. 223, Plenum, New York (1976).
13. N. OTSUKA, H. SATO, T. Y. TSENG, AND R. W. VEST, *J. Solid State Chem.* **53,** 290 (1984).
14. J. B. LEWIS, M.S. thesis, Purdue University (1983).
15. D. R. WHITE, Ph.D. thesis, Purdue University (1985).
16. S. CHEN, D. R. WHITE, H. SATO, C. J. SANDBERG, AND H. R. HARRISON, "Proceedings of High Temperature Solid Oxide Electrolyte Conference, Brookhaven National Laboratory," Upton, New York, p. 121 (1983).
17. J. R. AKRIDGE AND J. H. KENNEDY, *J. Solid State Chem.* **29,** 63 (1979).
18. P. D. DERNIER, AND J. P. REMEIKA, *J. Solid State Chem.* **17,** 245 (1976).
19. W. L. ROTH AND R. WONG, *Mater. Res. Soc. Symp. Proc.* **41,** 301 (1985).
20. W. C. HAMILTON, *Acta. Crystallogr.* **18,** 502 (1965).
21. H. ENGSTROM AND J. C. WANG, *Solid State Ionics* **1,** 441 (1980).
22. H. ENGSTROM, J. B. BATES, W. E. BRUNDAGE, AND J. C. WANG, *Solid State Ionics* **2,** 265 (1981).
23. J. P. BOILOT, G. COLLIN, PH. COLOMBAN, AND R. COMES, *Phys. Rev. B* **22,** 5912 (1980).
24. F. S. GALASSO, "Structure and Properties of Inorganic Solids," p. 220, Pergammon, Elmsford, N.Y. (1970).
25. R. D. SHANNON AND C. T. PREWITT, *Acta. Crystallogr. B* **25,** 925 (1969).
26. C. R. PETERS, M. BETTMAN, J. W. MOORE AND M. D. GLICK, *Acta Crystallogr. B* **27,** 1826 (1971).
27. J. THERY AND D. BRIANÇON, *Compte. Rend.* **254,** 2782 (1962).
28. J. GALLUP, *J. Amer. Ceram. Soc.* **18**(5), 144 (1935).
29. J. B. BATES, H. ENGSTROM, J. C. WANG, B. C. LARSON, N. J. DUDNEY, AND W. E. BRUNDAGE, *Solid State Ionics* **5,** 159 (1981).
30. J. C. WANG, J. B. BATES, N. J. DUDNEY, AND H. ENGSTROM, *Solid State Ionics* **5,** 35 (1981).
31. H. SATO AND R. KIKUCHI, *J. Phys. C* **7,** 159 (1977).
32. W. L. ROTH, *Trans. Amer. Cryst. Assoc.* **11,** 51 (1975).
33. D. R. WHITE, S. CHEN, M. SANKARARAMAN, AND H. SATO, *Solid State Ionics*, in press.